Landslides (2019) 16:993–1001
DOI 10.1007/s10346-019-01168-w
Received: 23 January 2019
Accepted: 6 March 2019
Published online: 18 March 2019

Kaiheng Hu · Xiaopeng Zhang · Yong You · Xudong Hu · Weiming Liu · Yong Li

Landslides and dammed lakes triggered by the 2017 Ms6.9 Milin earthquake in the Tsangpo gorge

Abstract An Ms6.9 earthquake in the Yarlung Tsangpo gorge on November 18, 2017 caused more than 700 landslides concentrating along the gorge's great bend, and three dammed lakes. The location and area of the landslides are obtained by interpreting high-resolution satellite images before and after the earthquake. About 31.45 Mm^3 of sediment from the landslides are distributed in seven catchments that are highly susceptible to debris flows. In 2018, at least three large-scale glacier-debris flows happened at Sedongpu, one of the seven catchments, and blocked temporarily the main river twice. The subsequent inundation and outburst floods resulted in infrastructure and property losses extensively beyond the high-seismic-intensity zone. Increase in the frequency of debris flows is attributed to the instability of glaciers and sediment supply caused by the earthquake. Glacier-debris flows will remain active for a long period due to massive glacial till, abundant rainfall, and meltwater. Geomorphic hazard chain triggered by such a mid-strong earthquake demonstrates that although coseismic landslides only occur in a limited area, the space and duration of the quake-induced hazards could extend largely under special geographical conditions.

Keywords Coseismic landslides · Dammed lakes · Outburst flood · Debris flow · Milin earthquake

Introduction

Strong earthquakes often cause various geomorphic hazard processes, for instance, large-scale landslides and dammed lakes in high mountain areas (Hu et al. 2017). Many such hazardous processes have been well documented since the last century such as the 1911 Usoi landslide and Lake Sarez by a Pamir earthquake in southeastern Tajikistan (Schuster and Alford 2004), the Yinping landslide and Lake Diexi by the 1933 Diexi earthquake in southwestern China (Costa and Schuster 1988; Chai et al. 1995), the 1970 Huascarán ice-rock falls and follow-up debris flows by an offshore earthquake in Peru (Evans et al. 2009), and the numerous landslides and dammed lakes by the 2008 Wenchuan earthquake in Sichuan, China (Cui et al. 2009, 2011).

It is commonly recognized that the location and scale of quake-induced geo-hazards are mainly controlled by the earthquake's seismogenic fault, magnitude, and local geological and geomorphic settings (Kargel et al. 2016). For example, the landslides caused by the 2008 Wenchuan earthquake mainly concentrated within a distance of 10 km to the seismogenic fault, and were particularly on the fault's hanging wall (Huang and Li 2008; Cui et al. 2011). The magnitude and scale of the quake-induced geo-hazards are far greater than that of those induced by other causes. The landslide area after the 1999 Chi-chi earthquake was three times prior to the quake in the Chenyulan basin of Taiwan (Lin et al. 2004). Worldwide inventory data of the quake-induced landslides show some logarithmic relationships between the earthquake magnitude and the landslide properties such as area and number (Keefer 1984, 2002).

However, there are limitations on space or life period for coseismic geo-hazards. Xin and Wang (1999) concluded that the earthquakes that can trigger landslides on natural slopes should be bigger than Ms4.7, and there are few coseismic landslides lied in the seismic zones of < VI degree. But, due to some extensive hazards such as dammed lakes or debris flows, the spatial and temporal dimensions of the coseismic hazards largely extend. Multi-hazard chains caused by earthquakes, such as the outburst flood of Diexi lake and the 1970 Huascarán debris flows, evolve at larger spatial and temporal scales, and impose greater threats on human beings lived outside the dangerous zone of the earthquake (Chai et al. 1995; Evans et al. 2009).

On 18 November 2017, an Ms6.9 earthquake happened in the depopulated zone of Tsangpo gorge, Pai Town, Milin county, Xizang (Tibet) Autonomous Region (epicenter 29.75° N, 95.02° E, focal depth 10 km). According to the China Earthquake Administration, the maximum intensity (VIII degree) region is about 310 km^2. The center of the earthquake zone is the Tsangpo gorge, the deepest gorge in the world where the Yarlung Tsangpo cuts a maximum depth of 6 km, and drops 2000 m over a reach of 200 km. It is also the most sensitive region in the world to climate change with rapid tectonic uplift. The coupling of special geo-environment of high mountains aggravates the effects of the earthquake-induced geo-hazards. In this paper, the landslides and dammed lakes caused by the Milin earthquake are interpreted with pre- and post-quake satellite images, and their control factors are presented. A series of blockage and breach events happened after the earthquakes, and the resulted lake outburst floods influenced farther downstream to India. This case shows how a mid-strong earthquake happened in a depopulated zone can bring damages to an extensive region in a long period.

Study area

This study focuses on the area in the river of Yarlung Tsangpo, with quake intensity higher than VII degree, about 2050 km^2, located in the eastern Himalayas, Tibet, China. It has unique geomorphological features of high mountain valleys with hillslopes of 25°~50°, deeply incised gorge, and the great bend (Fig. 1). The elevation ranges from 750 m a.s.l at Medog to 7782 m a.s.l at Namche Barwa massif. The river runs from west to east and then to south, at an average gradient of about 12.2‰.

The grand gorge is the largest water vapor channel on the edge of Tibetan Plateau. The warm and humid monsoon from the Indian Ocean makes it one of the highest rainfall areas in the world, from the peak of the glaciers and permanent snow to the valley of the tropical, constituting a vertical zone. The annual rainfall is as high as ca. 4000 mm in the southern part of the gorge, and between 1500 and 2000 mm in the northern part. Heavy rain is mainly concentrated in summer. The entire area is therefore extremely humid. It is full of dense forests and forms the most diverse biodiversity in the world. Majority of the study area has no

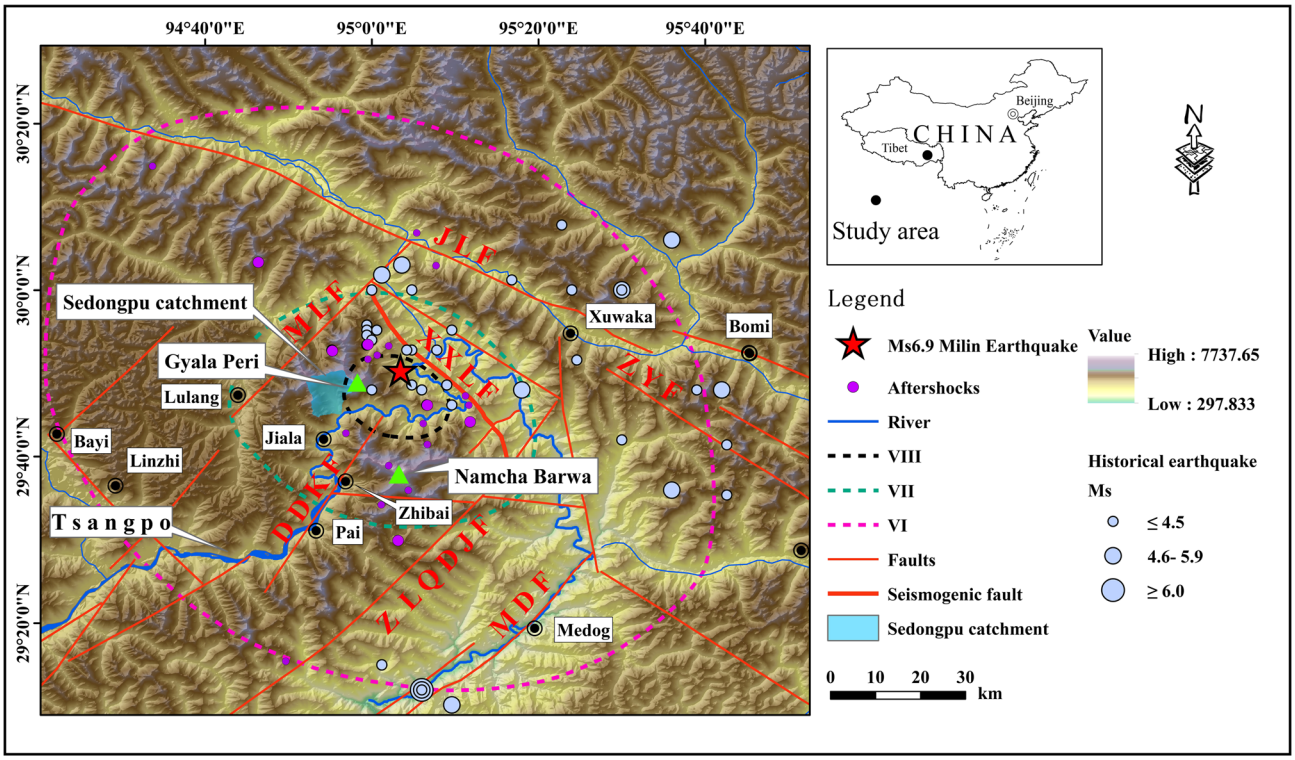

Fig. 1 The location map of the Milin earthquake and historical earthquakes near the Tsangpo gorge since 1950 (MLF, Milin fault; JLF, Jiali fault; ZYF, Zayu fault; XXLF, Xixingla fault; DDKF, Daduka fault; ZLQDJF, Zanda-Lahu-Qiduojiang fault; MDF, Medog fault)

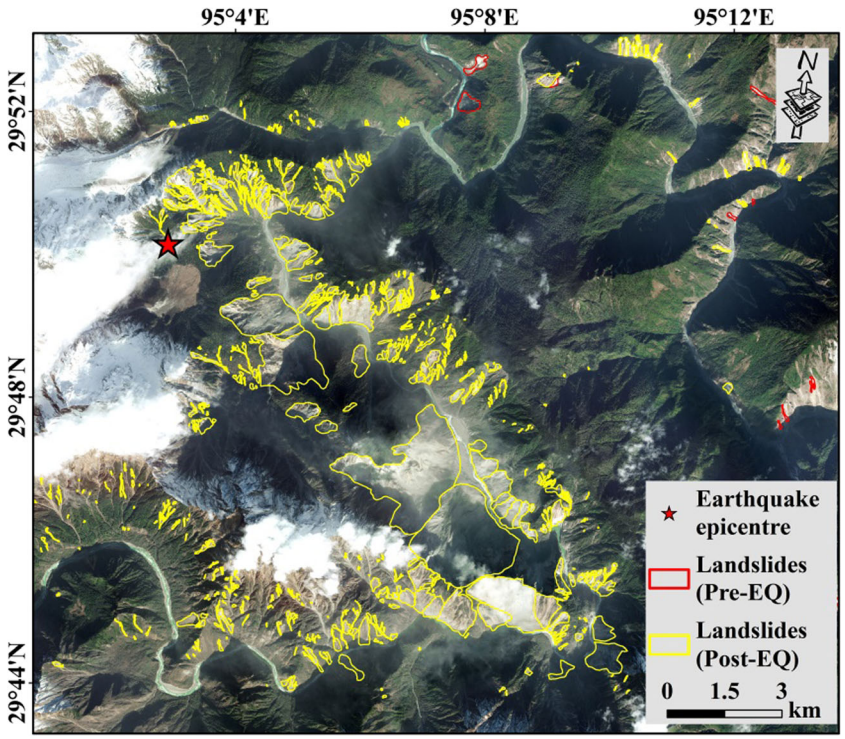

Fig. 2 Distribution of landslides induced by the Milin earthquake

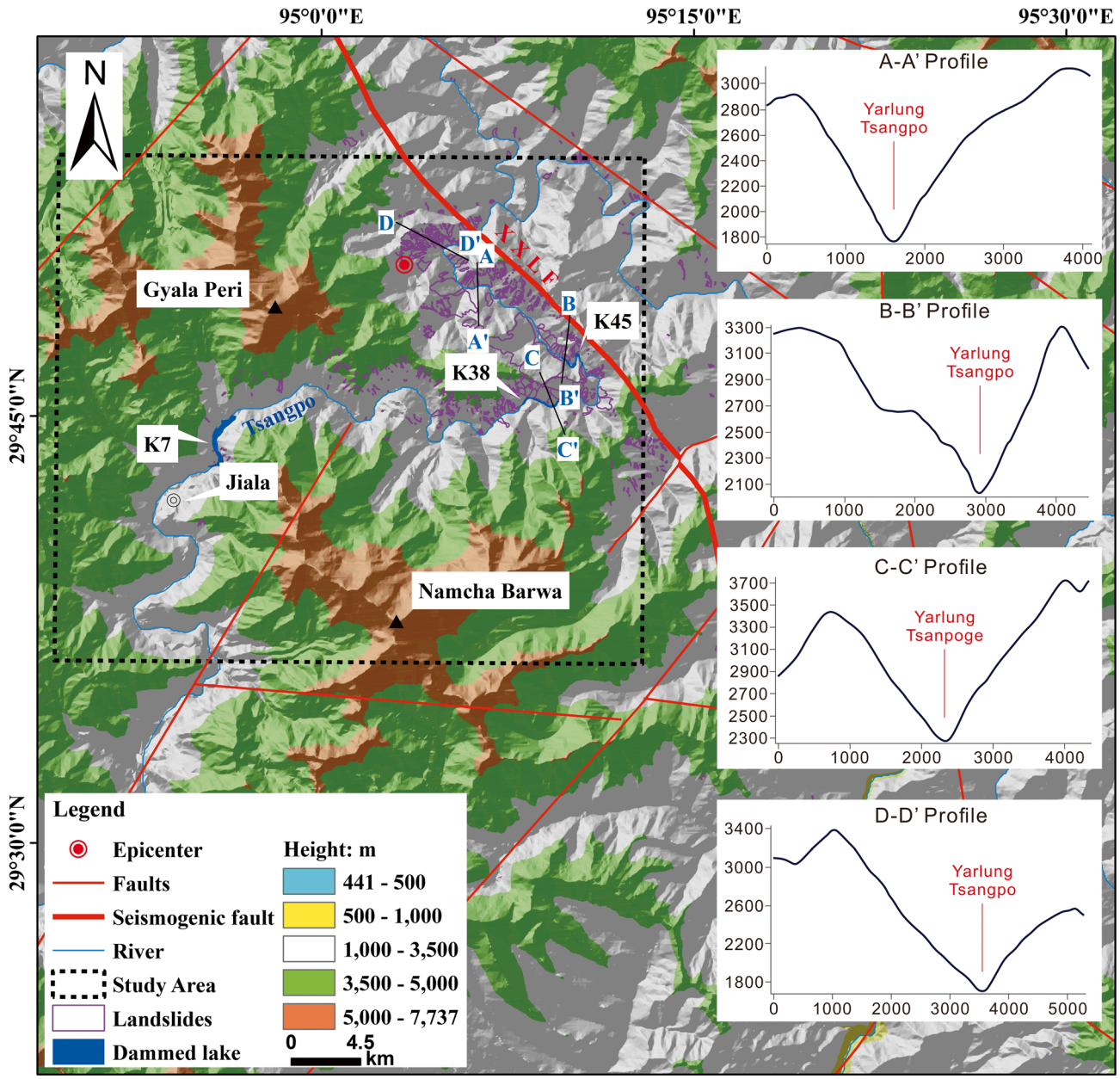

Fig. 3 Elevation distribution map of landslides and four profiles of the gorge where the concentrated area of landslides is (K7, K38, and K45 point to the three blockage sites shown in Fig. 4)

habitant, and the closest settlement to the epicenter and the great bend is the Jiala village.

The area can be divided into three units: the Namche Barwa metamorphic body, the Yarlung Tsangpo suture zone, and the Gangdese-Lhasa block (Zhang et al. 1992). The noticeable tectonic structure is the Namche Barwa syntaxis, the eastern tip of the interaction between the India plate and the Eurasian plate. It is a huge composite antiformal structure and has a complex geological structure. The left side of the antiform structure is bounded by the Milin-Lulang fault, and the right side is bounded by the Aniqiao-Medog fault (Zhang et al. 1992; Burg et al. 1998; Xu et al. 2008). Around the structures are a large number of small-scale faults and active faults, with frequent seismic activities (Fig. 1). It is a seismic zone in the southern part of the Qinghai-Tibet Plateau; the frequency of earthquakes is relatively high, most are moderate-strong, and seismic intensity is VII–VIII degrees. According to China Seismic Information, 67 recorded earthquakes ($Ms \geq 3.0$) were distributed near the study area since 1950, including the Medog 8.6 earthquake with the focal depth of 15 km happened at 14:09:34 UTC on 15 August 1950 near the China-India border (also

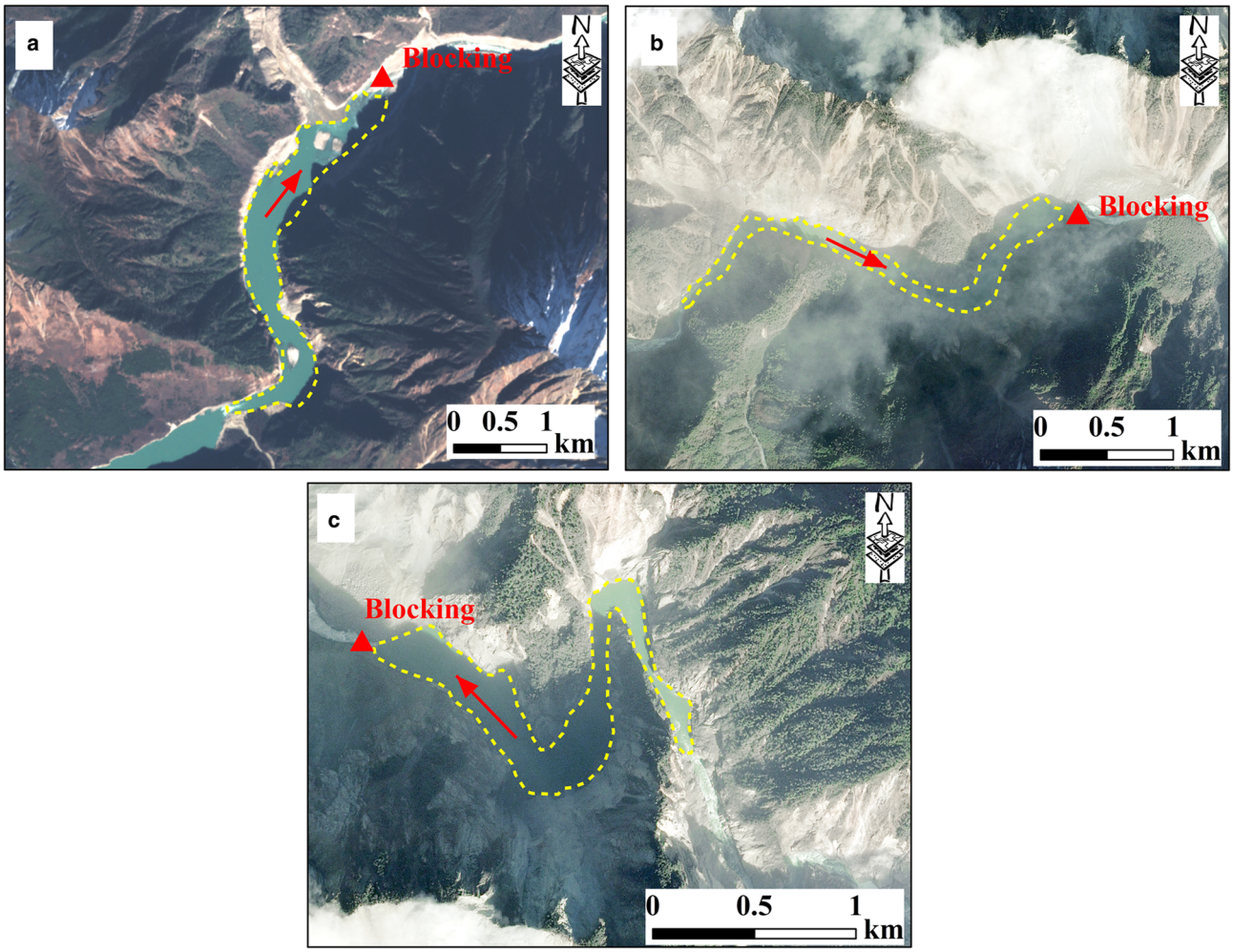

Fig. 4 The satellite remote sensing images of three dammed lakes. **a** K7 lake identified with the Sentinel 2 image of 9.4 m resolution; K38 (**b**) and K45 (**c**) lakes identified with the Spot 7 image of 1.3 m resolution (the red arrow is the flow direction, and the triangles are the blockage sites at which the dams were partially breached at that time)

known as the great Assam in India) (Chen and Molnar 1977) (Fig. 1). The regional fractures are located in the coseismic and post-earthquake coulomb stress-increasing regions caused by the Nepal earthquake in 2015, and there is still the possibility of occurrence of moderate-strong earthquakes in the later period.

The main outcrops in the epicenter area are the Namcha Barwa rock group, mainly composed of schist, gneiss, granulite, and other metamorphic rocks. The rock mass is broken and its stability is poor because of the strongest tectonic stress, the highest uplift and exfoliation rate in the Himalaya orogenic belt, the strongest metamorphism, and deep-melting effect in the Cenozoic (Xu et al. 2008). There are also widespread Quaternary glacial till, slope wash, and colluvium.

Coseismic landslides and dammed lakes

The Milin earthquake

The Ms6.9 Milin earthquake was the third largest magnitude in the study area since 1950. Its epicenter is located in the Bomi-Medog active structural belt, and the seismogenic fault is the NW-SE Xixingla fault (Fig. 1), surrounded by active thrust faults such as the Nujiang fault in the northwest, the Jiali fault, the Aparon fault, the NE-NNE Milin fault, the Medog fault, and the Yarlung Tsangpo fault, and some of them are accompanied by a large slip rate (Yin et al. 2018).

The earthquake affected six counties including Milin, Bayi, Medog, Chayu, Bomi, and Gongbo'gyamda. More than 12,000 were affected; some of the infrastructures such as houses (about 3000 houses), roads, communication lines, flood prevention embankments, and irrigation canals were damaged to some extent, but only three people were slightly injured. The earthquake induced a series of secondary hazards such as collapses, landslides, and debris flows, which caused multiple streamway blockages and dammed lakes. The great bend in the Tsangpo gorge was the worst-hit areas and the secondary hazards were mainly distributed in this area.

Coseismic landslides

The Milin earthquake has triggered a large number of rock/soil slides and collapses, which were identified by interpreting high-

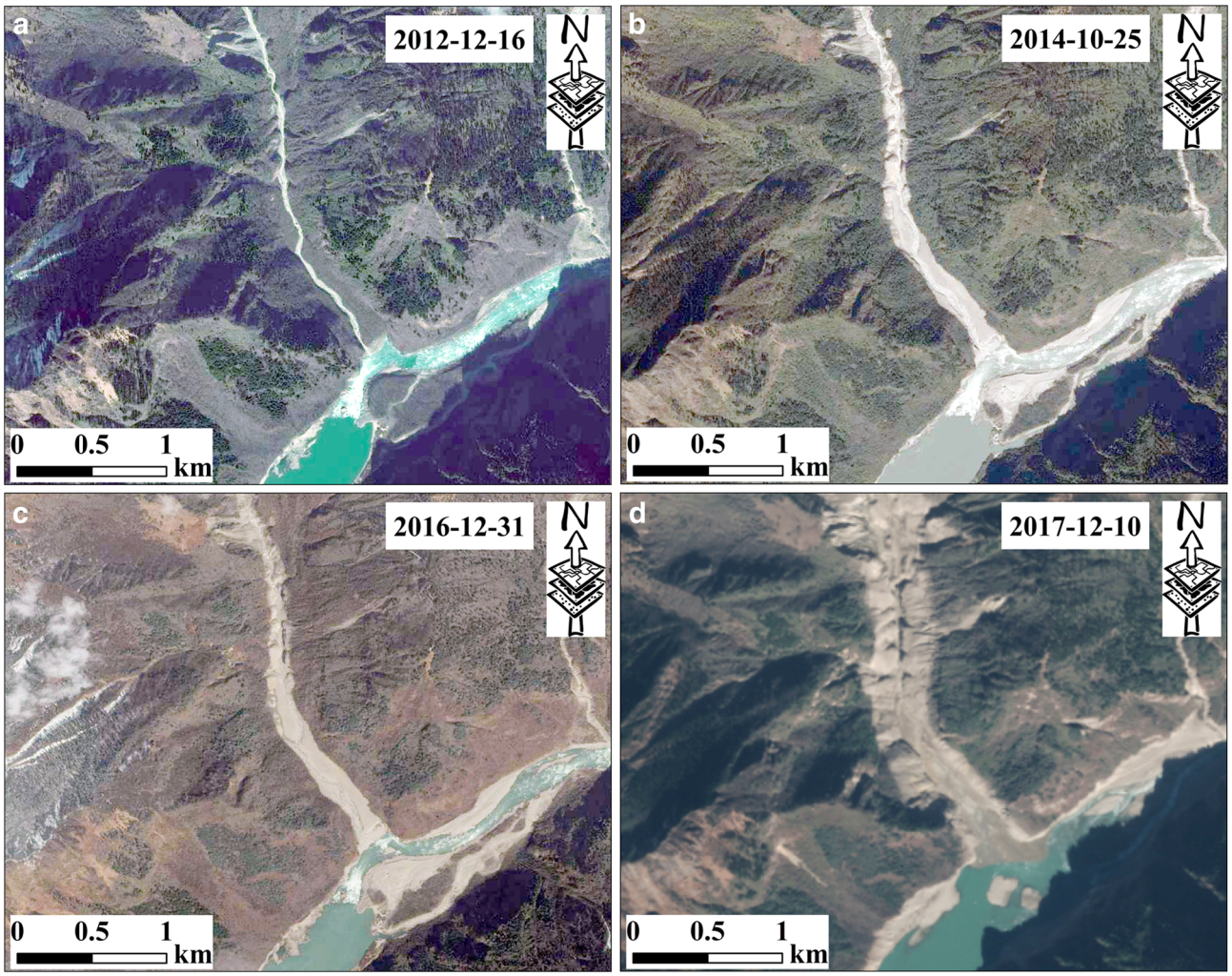

Fig. 5 Multi-temporal remote sensing image comparison (the satellite images in 2012, 2014, and 2016 were obtained from Google Earth, and the image in 2017 was from Sentinel)

resolution remote sensing images, including post-earthquake satellite images from Spot 7 with 1.3 m resolution and Sentinel with 9.4 m resolution, and pre-earthquake satellite images from Landsat 7 ETM with 15 m resolution and Google Earth. Due to high coverage of the vegetation, visual interpretation method was used to identify the coseismic hazards in the proximity of the epicenter. Nine hundred thirty-nine landslides were identified, covering an area of 37.65 km^2 (Fig. 2). Among them, 766 landslides with an area of 33.61 km^2 were attributed to by the Milin earthquake by comparing the satellite images before and after the quake (Landsat 7 ETM on Nov. 5, 2017 and Spot 7 on Dec. 12, 2017). Most landslides were shallow and small, distributed in clusters. The largest cluster of landslides covers an area of about 4.9 km^2, the minimum is 62.79 m^2, and the mean area is about 0.05 km^2. Limited by image accuracy, it is difficult to identify smaller areas of landslides. The total landslide volume (V) was calculated by the power-law landslide area-volume scaling relationship ($V = \alpha A^{\gamma}$) proposed by Larsen et al. (2010), where α is area-volume correction factor and γ is empirical index, respectively, and A is landslide area. The parameters in the scaling relationship are mainly affected by landslide type and geo-materials. The empirical index for shallow soil landslides is about 1.1–1.3, and for bedrock landslides with a deep scar area has a larger value ($\gamma = 1.3$–1.6). Considering the landslides in the study area are almost soil landslides, we adopt the global soil landslide parameters ($\log\alpha = -0.44$, $\gamma = 1.145$) from Larsen et al. (2010) as the empirically calibrated scaling parameters. It is roughly estimated that there was an increase of 0.085 km^3 in the total volume of loose materials. More accurate estimation of the total volume requires detailed field investigation.

The distribution of coseismic landslides is correlated with seismic, topographic, and geologic factors (Keefer 2002; Fan et al. 2017). The three factors play different roles in the landslide distribution in the study area. More than 90% of the landslides occurred at the great bend of the east structural knot of the Himalayas (Fig. 2), located in the leading edge area where the Indian plate and the Eurasian plate collide strongly and the geological body is significantly deformed (Yin and Harrison 2003). Poor stability of the stratum is because of the wide distribution of fractures and Namcha Barwa metamorphic rock group. Landslides are distributed in the middle mountain area (a.s.l. 1000~3500 m), and a small

Table 1 The basic information of the earthquake-triggered dammed lakes

Number	Longitude	Latitude	Lake area (km^2)	Estimated water depth (m)	Water level (m)	Volume (m^3)	Dam parameters Width (m)	Length (m)	Height (m)
K7	94° 55′ 58.8″ E	29° 45′ 18.0″ N	2.40	21.00	2766	0.77×10^7	302.00	2259.00	21.00
K38	95° 09′ 21.6″ E	29° 45′ 28.8″ N	0.92	58.00	2340	2.70×10^7	335.00	1418.00	48.00
K45	95° 10′ 37.2″ E	29° 47′ 16.8″ N	0.58	89.00	2120	3.10×10^7	482.00	3325.00	71.00

amount is distributed in the high mountain area (a.s.l. 3500~5000 m). The concentrated distribution of the landslide is an incised cut canyon with a V-shaped profile and steep slopes on both sides (Fig. 3). Earthquake-triggered landslides are mainly distributed on both sides of the canyon, especially at U-turns, not primarily along the seismogenic fault. The slopes on both sides of the river erosion form a temporary surface, and the steep terrain is easy to form a landslide under the action of ground motion. Moreover, the scour action, strong erosion, and the amplification effect on the seismic waves are conducive to the distribution of the landslides clustered on both sides of the Tsangpo gorge near the epicenter, and high landslide density in this area.

Accumulation and dam blockage

Nine landslide dams and three large earthquake-induced dammed lakes are identified in the valley section of Tsangpo, which formed in the Milin and the historical earthquakes. It is sure that the 1950 Assam earthquake caused some of the old landslides and dams. Zhang (1985) documented a large-scale glacier-debris flow event in the evening on 15 August 1950 triggered by the Assam earthquake. The event happened at Zelongnong catchment 20 km upstream of Jiala village, destroyed the Zhibai village at the foot of Namcha Barwa (Fig. 1), and blocked the Tsangpo river. The three lakes are located at 7 km (K7), 38 km (K38), and 45 km (K45) downstream of Jiala village respectively (Fig. 4). Among these, K7 dammed lake was formed by debris flows before the earthquake in November 2017; the other two dammed lakes K38 and K45 were formed by the earthquake-induced landslides. The latter two dams were overtopped shortly after the 2017 earthquake, and the lake storage capacity was not large (Fig. 4).

Many debris flows happened in the study area before the earthquake. Over the past decades, several debris flow events occurred in Sedongpu catchment adjacent to K7 lake which is located between the Gyala Peri massif (7294 m) and Namcha Barwa massif (Fig. 5). Glacier instability, meltwater, and local storms are the primary causes of these events. The drainage area, length of the main stream, and the average gradient of the catchment are approximately 66.7 km^2, 8.75 km, and 395‰, respectively. The relative relief is 4544 m from the Gyala Peri massif to the outlet at 2750 m a.s.l. to the Tsangpo. There are 16 glaciers with the total area of 23.6 km^2 and plenty of till in the area higher than 3600 m a.s.l. It is estimated that the Milin earthquake increases a volume of 3.3 Mm^3 sediment by the coseismic landslides.

As shown in Fig. 5, according to the analysis of the remote sensing image from Google Earth on December 16, 2012, December 31, 2013, and October 25, 2014, a large-scale debris flow occurred in the catchment during 2013 to 2014. The height of the muddy mark and mean channel slope of the event are obtained from the topographical map and satellite images. And based on the cross-sectional method, the overall debris flow volume was approximately 4.5 million m^3, briefly blocking Tsangpo. Based on further interpretation of Sentinel remote sensing image on December 10, 2017 and Spot7 remote sensing data on December 12, 2017, a large-scale debris flow event occurred in 2017, with a total of approximately 13 million m^3. The debris flow deposits blocked the river and formed a dammed lake of 1.48 km^2 (K7). And the elevation of the water level was about 2766 m (from Google Earth), currently.

Based on the results of the visual interpretation and the DEM with a resolution of 15 m, the geometric size parameters of the three dammed lakes were estimated, preliminarily. All dam shapes were controlled by the shape of the canyon and are elongated (Table 1). We used the GIS software to estimate the volume of the reservoir water, inundated area, and water depth in front of the dams. In the calculation process, the maximum water level of K7, K38, and K45 were 2766 m a.s.l., 2340 m a.s.l., and 2120 m a.s.l. respectively. According to preliminary estimates, in December 2017, the area of K7 dammed lake was 2.40 km^2, and the total water volume was about 0.77×10^7 m^3, and with a water depth of about 21 m; the lake K38 was about 0.92 km^2, and the water volume was about 2.70×10^7 m^3, and with a water depth of about 58 m; K45 dammed lake area was about 0.58 km^2, and the water volume was about 3.10×10^7 m^3, and with a water depth of about 89 m.

Later glacier-debris flows and dammed lakes

Due to large river gradient and high hydropower, the three dammed lakes naturally overflow shortly after the earthquake and no local people reported their existence. However, the earthquake triggered many landslides in the seven catchments on the left bank of the Tsangpo, and yielded a total volume of 31.45 Mm^3 of loose materials in them (Table 2, Fig. 6). These loose materials are likely to form large-scale debris flows due to ice and snow melting water in spring and heavy rainfalls in summer. Hu et al. (2018) predicted that the near-future large-scale debris flows would increase the height of the dams and the lake storage capacity, and warned of the danger of dammed lake outburst floods.

Table 2 Seven catchments with massive sediment supplies from the earthquake

Number	Longitude	Latitude	Watershed area (km^2)	Main stream length (m)	Gradient	Sediment increment (Mm^3)
1#	94° 56′ 12.45″	29° 45′ 2.91″	66.7	8.75	0.139	3.3
2#	94° 57′ 0.63″	29° 45′ 26.04″	4.22	3.20	0.267	0.06
3#	94° 58′ 22.61″	29° 45′ 40.3″	4.44	2.32	0.281	0.16
4#	94° 59′ 33.28″	29° 46′ 16.28″	14.29	4.05	0.346	1.71
5#	95° 7′ 6.72″	29° 45′ 8.3″	2.20	1.96	0.386	0.2
6#	95° 8 ′40.39″	29° 47′ 53.67″	6.37	3.65	0.203	17.57
7#	95° 5′ 50.78″	29° 49′ 30.3″	25.35	6.27	0.200	8.45

A large glacier-debris flow event occurred at Sedongpu around 5 a.m. on 17 October according to the official Xinhua news. But, the exact occurrence time is not unanimous, and two seismographic stations nearby recorded strong non-seismic wave signals at 22: 48 on the previous day. The mass of ice and debris covered and made up the residual dam at the same location in Fig. 4a, and completely blocked the Tsangpo. The accumulation area was 0.83 Mm^2, and the lowest point on the dam crest was about 80 m high. If the average depth of the accumulation was half of the height, the total volume of the deposited sediment was up to 33.2 Mm^3. Of course, the volume is the sum of several previous debris flow events. The maximum water level was 2830 m a.s.l at upstream Jiala village, and the impoundment was up to 0.6 billion m^3 when the right part of the dam began to overtop at 13:30 (Beijing time) on October 19 (Fig. 7). The peak discharge of the outburst flood was 23,400 m^3/s measured at 23:40 by Dexing hydrological station 180 km downstream of the dam. Just 10 days after the dam breach, a smaller debris flow occurred at Sedongpu and blocked the river again. The maximum impoundment was 0.32 billion m^3 at 9:30 a.m. on 31 October when the new dam was breaching.

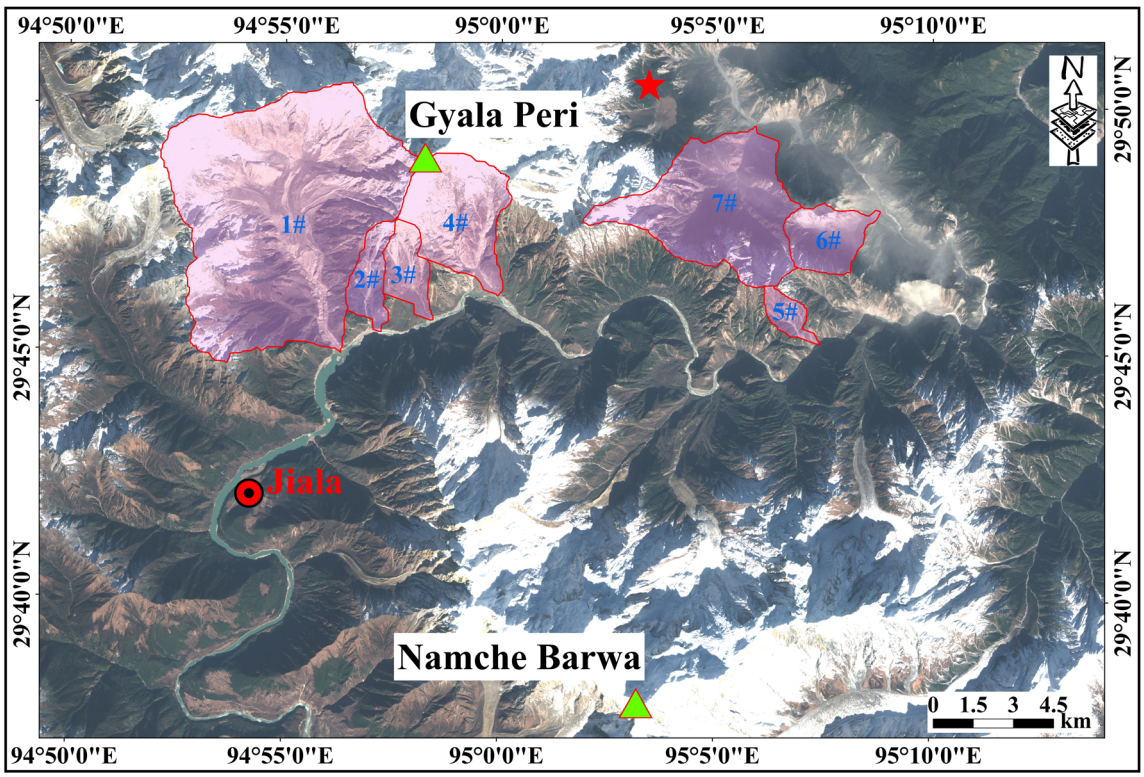

Fig. 6 The seven catchments with massive sediment supply and in high risk (the no. 1 is the Sedongpu catchment)

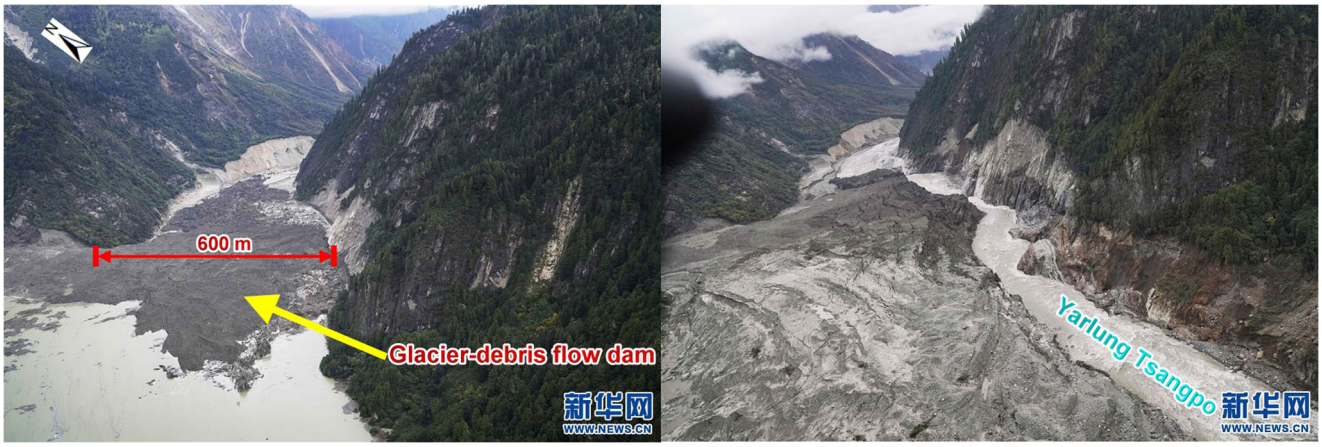

Fig. 7 The photos of the glacier-debris flow dam before and after the breach on October 19 taken by news reporters of the Xinhua News Agency from a helicopter

Conclusions

Interpretation of multi-temporal high-resolution satellite images shows that the 2017 Milin earthquake triggered 766 landslides with a total area of 33.61 km^2 and an estimated volume of 0.085 km^3 on both sides of Tsangpo gorge around the epicenter. The landslides caused nine temporary dams and three large dammed lakes in the trunk river shortly after the quake. The dammed lakes overflowed rapidly due to the steep gradient of the main river. But, in 2018, the rivers were completely blocked twice by several glacier-debris flows at Sedongpu catchment. The 2018 dammed lake inundated upstream highways and bridges, and its outburst flood made damages to downstream hydraulic engineering.

The Milin earthquake shows an example of how local topography strongly affects the spatial distribution of earthquake-induced landslides. The coseismic landslides spatially distribute along both sides of the gorge, especially on the U-turn reach, but not along the seismogenic fault. Trunk river incision generates free surfaces and steep hillslopes that are susceptible to quake-induced landslides. The earthquake not only provides a great amount of loose materials for debris flows, but also aggravates the instability of glaciers near the epicenter. During the almost 40 years before the 2017 earthquake, there were two glacier-debris flow events at Sedongpu. However, at least three events happened just in 10 months after the earthquake and blocked the Yarlung Tsangpo. The increase in the frequency and scale of debris flows may result from the unstable glaciers and coseismic landslides. Furthermore, the activity of glacier-debris flows will last a long time due to massive glacial till, abundant rainfall, and meltwater. But, for different types of events, the meltwater and rainfalls may play different roles in the initiation of debris flows.

The influence period of earthquake-induced geo-hazards is prolonged greatly by the gorge's special geomorphic settings. Although these dammed lakes have overtopped, the upstream and downstream areas are still in the high risk of future glacier-debris dammed lakes. Hence, it is necessary to assess the potential danger of future dammed lakes in the Tsangpo gorge, especially in reaches near the seven high-risk catchments based on further field geo-environmental surveys. Non-structural countermeasures such as monitoring and warning systems and evacuation plans are suitable for dealing with future hazards.

Funding information This work has been supported by the National Natural Science Foundation of China (Grant No.91747207 and 41790434) and the Research and Demonstration Program of Precise Warning and Emergence Disposal Technologies against geo-hazards in Jiuzhaigou scenic area (Grant No.KJ-2018-23).

References

Burg JP, Nievergelt P, Oberli F, Seward D, Davy P, Maurin JC, Diao Z, Meier M (1998) The Namche Barwa syntaxis: evidence for exhumation related to compressional crustal folding. J Asian Earth Sci 16(2–3):239–252

Chai HJ, Liu HC, Zhang ZY (1995) Landslide dams induced by Diexi earthquake in 1933 and its environmental effect. J Geol Hazard Environ Preserv 6(1):7–17 (in Chinese)

Chen WP, Molnar P (1977) Seismic moments of major earthquakes and the average rate of slip in central Asia. J Geophys Res 82(20):2945–2969

Costa JE, Schuster RL (1988) Formation and failure of natural dams. Geol Soc Am Bull 100(7):1054–1068

Cui P, Zhu Y, Han Y, Chen XQ, Zhuang JQ (2009) The 12 May Wenchuan earthquake-induced landslide lakes: distribution and preliminary risk evaluation. Landslides 6(3):209–223. https://doi.org/10.1007/s10346-009-0160-9

Cui P, Chen XQ, Zhu YY, Su FH, Wei FQ, Han YS, Liu HJ, Zhuang JQ (2011) The Wenchuan earthquake (May 12, 2008), Sichuan province, China, and resulting geohazards. Nat Hazards 56(1):19–36

Evans SG, Bishop NF, Smoll LF et al (2009) A re-examination of the mechanism and human impact of catastrophic mass flows originating on Nevado Huascarán, Cordillera Blanca, Peru in 1962 and 1970. Eng Geol 108(1–2):96–118

Fan X, Xu Q, Van Westen CJ, Huang R, Tang R (2017) Characteristics and classification of landslide dams associated with the 2008 Wenchuan earthquake. Geoenvironmental Disasters 4(1):12. https://doi.org/10.1186/s40677-017-0079-8

Hu K, Chen X, Ge Y, Jiang X, Wang Y (2017) Landslides triggered by the Ms6.5 Ludian, China earthquake of August 3, 2014. In: Mikoš M, Casagli N, Yin Y, Sassa K (eds) Advancing culture of living with landslides. WLF 2017. Springer, Cham

Hu K, Zhang X, Tang J, Liu W (2018) Potential danger of dammed lakes induced by the 2017 Ms6.9 Milin earthquake in the Tsangpo gorge. 5th International Conference Debris Flows: Disasters, Risk, Forecast, Protection, pp 97–104

Huang R, Li WL (2008) Research on development and distribution rules of geohazards induced by Wenchuan earthquake induced by Wenchuan earthquake on 12th May, 2008. Chin J Rock Mech Eng 27(12):2585–2592

Kargel JS, Leonard GJ, Shugar DH, Haritashya UK, Bevington A, Fielding EJ, Fujita K, Geertsema M, Miles ES, Steiner J, Anderson E, Bajracharya S, Bawden GW, Breashears DF, Byers A, Collins B, Dhital MR, Donnellan A, Evans TL, Geai ML, Glasscoe MT, Green D, Gurung DR, Heijenk R, Hilborn A, Hudnut K, Huyck C, Immerzeel WW, Liming J, Jibson R, Kaab A, Khanal NR, Kirschbaum D,

Kraaijenbrink PDA, Lamsal D, Shiyin L, Mingyang L, McKinney D, Nahirnick NK, Zhuotong N, Ojha S, Olsenholler J, Painter TH, Pleasants M, Pratima KC, Yuan QI, Raup BH, Regmi D, Rounce DR, Sakai A, Donghui S, Shea JM, Shrestha AB, Shukla A, Stumm D, van der Kooij M, Voss K, Xin W, Weihs B, Wolfe D, Lizong W, Xiaojun Y, Yoder MR, Young N (2016) Geomorphic and geologic controls of geohazards induced by Nepal's 2015 Gorkha earthquake. Science 351(6269):aac8353

Keefer DK (1984) Landslides caused by earthquakes. Geol Soc Am Bull 95(4):406–421

Keefer DK (2002) Investigating landslides caused by earthquakes–a historical review. Surv Geophys 23(6):473–510

Larsen IJ, Montgomery DR, Korup O (2010) Landslide erosion controlled by hillslope material. Nat Geosci 3(4):247–251

Lin CW, Shieh CL, Yuan BD, Liu SH, Lee SY (2004) Impact of Chi-Chi earthquake on the occurrence of landslides and debris flows: example from the Chenyulan River watershed, Nantou, Taiwan. Eng Geol 71(1):49–61

Schuster RL, Alford D (2004) Usoi landslide dam and Lake Sarez, Pamir Mountains, Tajikistan. Environ Eng Geosci 10(2):151–168

Xin HB, Wang YQ (1999) Criteria for earthquake-induced landslide and avalanche. Chin J Geotech Eng 21(5):591–594 (in Chinese)

Xu GQ, Cai ZF, Zhang ZM, Li HQ, Chen FY, Tang ZM (2008) Tectonics and fabric kinematics of the Namche Barwa terrane, Eastern Himalayan Syntaxis. Acta Petrol Sin 24(7):1463–1476 (in Chinese)

Yin A, Harrison TM (2003) Geologic evolution of the Himalayan-Tibetan orogen. Annu Rev Earth Planet Sci 28(28):211–280

Yin FL, Han LB, Jiang CS, Shi YL (2018) Interaction between the 2017 M6.9 Mainling earthquake and the 1950 M8.6 Zayu earthquake and their impacts on surrounding major active faults. Chin J Geophys 61(8):3185-3197 (in Chinese)

Zhang WJ (1985) Some features of the surge glacier in the Mt. Namcha Barwa. Mt Res 3(4):234–238 (in Chinese)

Zhang ZG, Liu YH, Wang TW (1992) Geology of Namcha Barwa areas. Science Press, Beijing (in Chinese)

K. Hu (✉) · X. Zhang · Y. You · X. Hu · W. Liu · Y. Li
Key Laboratory of Mountain Hazards and Earth Surface Processes,
Chinese Academy of Sciences,
Chengdu, 610041, Sichuan, China
Email: khhu@imde.ac.cn

K. Hu · X. Zhang · Y. You · X. Hu · W. Liu · Y. Li
Institute of Mountain Hazards and Environment,
Chinese Academy of Sciences and Ministry of Water Conservancy,
Chengdu, 610041, Sichuan, China

X. Zhang · X. Hu
University of Chinese Academy of Sciences,
Beijing, 100049, China